

Beamforming Gain with Nonideal Phase Shifters

Heedong Do, *Member, IEEE*, Angel Lozano, *Fellow, IEEE*

Abstract—This research sets forth a universal framework to characterize the beamforming gain achievable with arbitrarily nonideal phase shifters. Precisely, the maximum possible shortfall relative to the gain attainable with ideal phase shifters is established. Such shortfall is shown to be fundamentally determined by the perimeter of the convex hull of the set of feasible beamforming coefficients on the complex plane. This result holds regardless of whether the beamforming is at the transmitter, at the receiver, or at a reconfigurable intelligent surface. In i.i.d. fading channels, the shortfall hardens to the maximum possible shortfall as the number of antennas grows.

Index Terms—Beamforming, digital beamforming, analog beamforming, equal-gain combining, convex geometry, convex hull, reconfigurable intelligent surface, fading channels

I. INTRODUCTION

Beamforming is a long-standing technique in wireless communication, instrumental to increase the received signal strength and/or extend the transmission range [1, Sec. 5.3]. The relevance of beamforming has only grown over time, as operating frequencies increase and the array dimensionalities surge to counter the associated propagation losses. In 6G, base stations could feature well over a thousand antennas in their arrays [2]. Beamforming will be a chief ingredient, and a complete understanding of its performance is thus of paramount importance.

The scope of this paper extends to any beamformer, analog or digital, at transmitter or receiver, that is implemented by shifting the signal’s phase at each antenna. For the sake of performance analysis, phase shifters are usually regarded as ideal, meaning that they can manipulate the phase unrestrictedly, with an infinite resolution, and without altering the signal’s magnitude. This ideality, however, does not hold in actuality because:

- For digital beamformers, the resolution is necessarily coarse [3, Table 2-5], and the maximum phase change is limited [3, Table 6].
- For analog beamformers, while the resolution is infinite, the range is again limited [3, p. 27].
- Insertion losses are not independent of the phase shift, which couples the phase and magnitude responses [4].

These and other non-idealities can be captured by defining a set (continuous or discrete) of feasible beamforming coefficients, and the question is then to quantify the beamforming gain when the coefficients are restricted to being drawn from this set. This paper tackles this question, with the key findings being that:

H. Do and A. Lozano are with Univ. Pompeu Fabra, 08018 Barcelona (e-mail: {heedong.do, angel.lozano}@upf.edu). Their work is supported the Maria de Maeztu Units of Excellence Programme CEX2021-001195-M funded by MICIU/AEI/10.13039/501100011033, and by the Departament de Recerca i Universitats de la Generalitat de Catalunya.

- For any given channel, the shortfall relative to ideal phase shifting of any arbitrary set of feasible beamforming coefficients is bounded.
- This worst-case shortfall is intimately related to the perimeter of the convex hull of the set of beamforming coefficients on the complex plane.
- In i.i.d. fading channels, as the number of antennas grows large the shortfall comes to equal this worse-case value.

The manuscript is organized as follows. The main result bounding the shortfall relative to ideal phase shifting is presented immediately in Sec. II, with its derivation following in Sec. III. Subsequently, Sec. IV provides an alternative derivation that is geometric in nature, and Sec. V shows how the main result can be tightened slightly at the expense of generality. Finally, Sec. VI concludes the paper.

II. MAIN RESULT

Consider a connection between an N -antenna array and a single antenna. Within the array, each antenna is able to apply a beamforming coefficient drawn from a compact set

$$\mathcal{W} \subset \{w \in \mathbb{C} : |w| \leq 1\}. \quad (1)$$

As a special case, an ideal phase shifter would correspond to

$$\mathcal{W}_{\text{ideal}} = \{w \in \mathbb{C} : |w| = 1\}. \quad (2)$$

Common sets, both continuous and discrete, are listed in Table I. In particular, and for future reference, the regular M -gon is denoted by

$$\mathcal{W}_M \equiv \left\{ e^{j2\pi \frac{0}{M}}, e^{j2\pi \frac{1}{M}}, \dots, e^{j2\pi \frac{M-1}{M}} \right\}. \quad (3)$$

Let h_n be the channel coefficient at the n th array antenna, such that

$$h_n = |h_n| e^{j\theta_n}, \quad (4)$$

and let w_n be the beamforming coefficient at the n th antenna. The beamforming gain is given by

$$\left| \sum_n w_n h_n \right|^2, \quad (5)$$

suitably normalized depending on the pertinent power constraint, which in turn depends on whether the beamforming is at a transmitter or receiver. For the sake of compactness,

$$g(\mathbf{w}) = \left| \sum_n w_n h_n \right| \quad (6)$$

is henceforth used in lieu of (5), with $\mathbf{w} \equiv (w_1, \dots, w_N)$.

For ideal phase shifters abiding by (2), the maximum value of (6) is, from the triangle inequality,

$$g_{\text{ideal}} = \sum_n |h_n| \quad (7)$$

TABLE I
COMMON SETS \mathcal{W} WITH THE SHADED REGIONS INDICATING THE CORRESPONDING CONVEX HULLS

Set						
References	-	[32]–[35]	[36]–[39]	[40]–[42]	[43]–[45]	[46]

* $\mathcal{W} = \{r(\theta)e^{j\theta} : r(\theta) = (1 - \beta)(\frac{1+\sin\theta}{2})^\alpha + \beta\}$, with the drawing corresponding to $\alpha = 2$ and $\beta = 0.5$.

achieved by $w_n = e^{-j\theta_n}$.

For arbitrary phase shifters, one can simply round each $w_n = e^{-j\theta_n}$ to \mathcal{W} [5]–[9]. This simplicity, though, comes with a penalty in beamforming gain. Such a penalty can be prevented by designs that, rather than rounding to \mathcal{W} , are based on it from the outset [10]–[19]. In fact, it turns out that the optimum \mathbf{w} for any arbitrary \mathcal{W} and h_1, \dots, h_N as well as the corresponding

$$g_{\mathcal{W}} = \max_{\mathbf{w} \in \mathcal{W}^N} \left| \sum_n w_n h_n \right| \quad (8)$$

can be efficiently computed without exhaustively searching over \mathcal{W}^N [20]–[31].

This paper uncovers a universal relationship between this optimum value with arbitrary phase shifters, $g_{\mathcal{W}}$, and its counterpart with ideal phase shifters, g_{ideal} . Specifically, it is established that

$$g_{\mathcal{W}} \geq \text{constant} \cdot g_{\text{ideal}} \quad (9)$$

with

$$\text{constant} = \frac{\text{perimeter of Conv } \mathcal{W}}{2\pi}, \quad (10)$$

where $\text{Conv}(\cdot)$ denotes the convex hull of a set. The shortfall in beamforming gain (in dB) associated with nonideal phase shifting is therefore, at most,

$$20 \log_{10} \left(\frac{\text{perimeter of Conv } \mathcal{W}}{2\pi} \right). \quad (11)$$

Note that, if \mathcal{W} does not reside on the unit circle, this shortfall subsumes a power loss

$$10 \log_{10} \left(\frac{1}{N} \sum_n |w_n|^2 \right). \quad (12)$$

Conversely, if \mathcal{W} does reside on the unit circle, then the shortfall is caused entirely by the limited range and resolution of the phase shifting.

The applicability of the above result is exemplified in Fig. 1. This applicability extends, besides point-to-point beamforming, to transmissions via a RIS. In that case, the role of the N array antennas is played by the N RIS elements and h_n signifies the channel coefficient linking transmitter and receiver through the n th such element. Also included are settings where, besides the transmitter-RIS-receiver connection, there is a direct transmitter-receiver path and the response

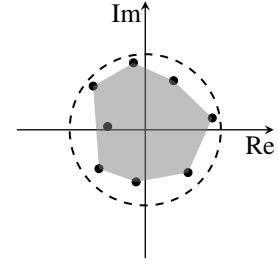


Fig. 1. Response of 3-bit phase shifter. The dots are the elements of \mathcal{W} while the shaded region is their convex hull. The dashed circle is $\mathcal{W}_{\text{ideal}}$. As the perimeter of the heptagonal convex hull equals 5.01, there exists some \mathbf{w} attaining $5.01/2\pi \approx 80\%$ of g_{ideal} , which corresponds to a 2-dB shortfall in beamforming gain. Part of this shortfall is the power loss caused by the magnitude of the elements of \mathcal{W} being less than unity.

coefficients at the RIS elements are drawn from \mathcal{W}_M : letting h_0 denote the direct path, the beamforming optimization

$$\max_{\mathbf{w} \in \mathcal{W}_M^N} \left| h_0 + \sum_n w_n h_n \right| = \max_{(\mathbf{w}_0, \mathbf{w}) \in \mathcal{W}_M^{N+1}} \left| w_0 h_0 + \sum_n w_n h_n \right| \quad (13)$$

is merely an augmented version of (8) (see App. A).

The relevance of the result also extends to fading channels, and in particular to $\{h_n\}$ drawn from any i.i.d. circularly symmetric distribution. If $\{h_n\}$ are i.i.d. realizations of h , then, as N grows large, the ideal beamforming gain (normalized by N^2 to keep it from diverging) converges to $(\mathbb{E}[|h|])^2$. Relative to it, the worst-case shortfall with an arbitrary set of phase shifts is again given by (11). In fact, in this large- N regime, the shortfall equals this worst-case value.

III. DERIVATION OF THE MAIN RESULT

This section lays down the derivation of (9)–(10), beginning with a presentation of the necessary mathematical machinery, chiefly the notion of support function.

A. The Support Function

Identifying \mathbb{C} with \mathbb{R}^2 , the inner product of two complex numbers can be defined as

$$\langle \cdot, \cdot \rangle : \mathbb{C} \times \mathbb{C} \rightarrow \mathbb{R} \quad (14)$$

$$(z, w) \mapsto \text{Re}\{\bar{z}w\}.$$

The workhorse of the analysis that follows is the identity

$$|w| = \max_{\theta \in [0, 2\pi]} \langle e^{j\theta}, w \rangle, \quad (15)$$

which turns a nonlinear function into the optimization of a linear one, whereby the beamforming optimization can be decoupled into

$$g_{\mathcal{W}} = \max_{\mathbf{w} \in \mathcal{W}^N} \left| \sum_n w_n h_n \right| \quad (16)$$

$$= \max_{\mathbf{w} \in \mathcal{W}^N} \max_{\theta \in [0, 2\pi]} \left\langle e^{j\theta}, \sum_n w_n h_n \right\rangle \quad (17)$$

$$= \max_{\mathbf{w} \in \mathcal{W}^N} \max_{\theta \in [0, 2\pi]} \sum_n \left\langle e^{j\theta}, w_n h_n \right\rangle \quad (18)$$

$$= \max_{\theta \in [0, 2\pi]} \sum_n \max_{w \in \mathcal{W}} \left\langle e^{j\theta}, w h_n \right\rangle \quad (19)$$

$$= \max_{\theta \in [0, 2\pi]} \sum_n |h_n| \max_{w \in \mathcal{W}} \left\langle e^{j(\theta - \theta_n)}, w \right\rangle. \quad (20)$$

The inner optimization problem in (20) is of the form $\max_{w \in S} \langle z, w \rangle$, hence the mapping

$$\begin{aligned} \mathbb{C} &\rightarrow \mathbb{R} \\ z &\mapsto \max_{w \in S} \langle z, w \rangle \end{aligned} \quad (21)$$

becomes of interest. This mapping, well defined because S is a compact set, depends only on the convex hull of S .

Lemma 1. For a compact set $S \subset \mathbb{C}$,

$$\max_{w \in S} \langle z, w \rangle = \max_{w \in \text{Conv } S} \langle z, w \rangle. \quad (22)$$

Proof. This is a special case of the result for convex functions in [49, Thm. 32.2]. \square

The mapping in (21) can be identified with the *support function* of $\text{Conv } S$ [50, Ch. 1.7]. A useful property of convex hull is provided next.

Lemma 2. For sets S_1 and S_2 in \mathbb{C} ,

$$\text{Conv}(S_1 + S_2) = \text{Conv } S_1 + \text{Conv } S_2. \quad (23)$$

Proof. See [50, Thm. 1.1.2]. \square

B. A Lower Bound

Let us next bound $g_{\mathcal{W}}$ on the basis that the maximum is at least the average and that the mapping

$$\theta \mapsto \max_{w \in \mathcal{W}} \langle e^{j\theta}, w \rangle \quad (24)$$

is periodic, with period 2π .

Theorem 1. The inequality in (9) holds with

$$\text{constant} = \frac{1}{2\pi} \int_0^{2\pi} \max_{w \in \mathcal{W}} \langle e^{j\theta}, w \rangle d\theta. \quad (25)$$

Proof. See App. B. \square

In the special case that $\mathcal{W} = \{0, 1\}$, it can be verified that

$$\max_{w \in \mathcal{W}} \langle e^{j\theta}, w \rangle = \max(\cos \theta, 0), \quad (26)$$

whose integral over $[0, 2\pi]$ equals 2. This turns Thm. 1 into

$$g_{\mathcal{W}} \geq \frac{1}{\pi} \sum_n |h_n|. \quad (27)$$

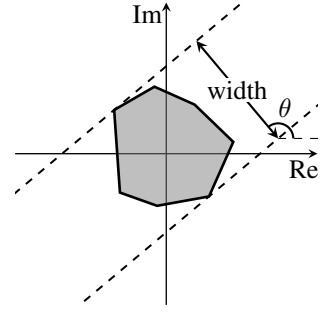


Fig. 2. Width of a convex set in the direction specified by θ .

In the context of RIS-assisted communication, a similar result is available in [33, Thm. 2], but only for $N \rightarrow \infty$ and under certain assumptions on the values that the channel can take. This special case, $\mathcal{W} = \{0, 1\}$, is further presented in [51]–[53], in the slightly different (but ultimately equivalent) form of showing that there exists a subset $S \subset \{1, \dots, N\}$ satisfying

$$\left| \sum_{n \in S} h_n \right| \geq \frac{1}{\pi} \sum_n |h_n|. \quad (28)$$

This formulation appears in various textbooks as an exercise [54, Ch. VIII, Exercise 3.1], [55, Exercise 14.9]. A weaker version with a constant $\frac{1}{6}$ appeared in the 1986 Chinese Mathematical Olympiad [56, pp. 23].

C. Geometric Interpretation

Results from convex geometry allow interpreting the constant in (25) geometrically. The width of a compact convex set $S \subset \mathbb{C}$ in the direction of θ is defined as [50, Sec. 1.7]

$$\max_{w \in \mathcal{W}} \langle e^{j\theta}, w \rangle + \max_{w \in \mathcal{W}} \langle e^{j(\theta+\pi)}, w \rangle \quad (29)$$

and illustrated in Fig. 2. The mean width of S is then

$$\begin{aligned} \frac{1}{2\pi} \int_0^{2\pi} \left(\max_{w \in \mathcal{W}} \langle e^{j\theta}, w \rangle + \max_{w \in \mathcal{W}} \langle e^{j(\theta+\pi)}, w \rangle \right) d\theta \\ = \frac{1}{\pi} \int_0^{2\pi} \max_{w \in \mathcal{W}} \langle e^{j\theta}, w \rangle d\theta \end{aligned} \quad (30)$$

from the periodicity of (24). One can relate this mean width with the perimeter of S using the Cauchy's surface area formula [50, Sec. 5.3], whose two-dimensional instance is presented next as Thm. 2; see [57], [58] for intuitive explanations. Application of the formula directly gives, as desired,

$$\frac{1}{2\pi} \int_0^{2\pi} \max_{w \in \mathcal{W}} \langle e^{j\theta}, w \rangle d\theta = \frac{\text{perimeter of } \text{Conv } \mathcal{W}}{2\pi}. \quad (31)$$

Theorem 2. (Cauchy's surface area formula) For a compact convex set $S \subset \mathbb{C}$,

$$\text{mean width of } S = \frac{\text{perimeter of } S}{\pi}. \quad (32)$$

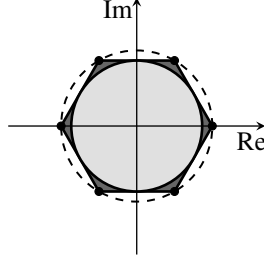


Fig. 3. Visual comparison of the constants in (33) and (10), which respectively correspond to the perimeter of the circle in light gray and to the perimeter of the regular M -gon in charcoal gray, both divided by 2π . As a reference, the unit circle is shown as a dashed line.

D. Comparison with an Existing Result

For the special case of $\mathcal{W} = \mathcal{W}_M$, the bound in (9) is available in [59, Prop. 2], albeit with the looser constant

$$\min_{\theta \in [0, 2\pi]} \max_{w \in \mathcal{W}_M} \langle e^{j\theta}, w \rangle = \cos \frac{\pi}{M}. \quad (33)$$

This result readily follows from (20) via

$$g_{\mathcal{W}} = \max_{\theta \in [0, 2\pi]} \sum_n |h_n| \max_{w \in \mathcal{W}_M} \langle e^{j(\theta - \theta_n)}, w \rangle \quad (34)$$

$$\geq \min_{\theta \in [0, 2\pi]} \sum_n |h_n| \max_{w \in \mathcal{W}_M} \langle e^{j(\theta - \theta_n)}, w \rangle \quad (35)$$

$$\geq \sum_n |h_n| \min_{\theta \in [0, 2\pi]} \max_{w \in \mathcal{W}_M} \langle e^{j(\theta - \theta_n)}, w \rangle \quad (36)$$

$$= \min_{\theta \in [0, 2\pi]} \max_{w \in \mathcal{W}_M} \langle e^{j\theta}, w \rangle \cdot \sum_n |h_n| \quad (37)$$

$$= \cos \frac{\pi}{M} \cdot g_{\text{ideal}}. \quad (38)$$

The constant in (33) is indeed looser than (10) because the average is at least the minimum, that is,

$$\frac{1}{2\pi} \int_0^{2\pi} \max_{w \in \mathcal{W}_M} \langle e^{j\theta}, w \rangle d\theta \geq \min_{\theta \in [0, 2\pi]} \max_{w \in \mathcal{W}_M} \langle e^{j\theta}, w \rangle. \quad (39)$$

As (33) is the radius of the circle inscribed in $\text{Conv } \mathcal{W}_M$, the inequality corresponds (see Fig. 3) to

$2\pi \cdot (\text{radius of the inscribed circle}) \leq \text{perimeter of } \text{Conv } \mathcal{W}$.

The difference between the constants in (33) and (10) can be conveniently quantified asymptotically. For large M , (33) expands as

$$1 - \frac{\pi^2}{2} \cdot \frac{1}{M^2} + O\left(\frac{1}{M^4}\right) \quad (40)$$

whereas, for a regular M -gon, (10) becomes¹

$$\frac{1}{2\pi} \cdot 2M \sin \frac{\pi}{M} = 1 - \frac{\pi^2}{6} \cdot \frac{1}{M^2} + O\left(\frac{1}{M^4}\right). \quad (41)$$

The latter approaches unity three times faster.

¹The expansion in (41) coincides with that of a phase quantization error in the array processing literature [60, Eqn. 75].

E. Tightness

As the next result formalizes, for Thm. 1 to hold for any N and h_1, \dots, h_N , the constant in (25) cannot be further tightened.

Theorem 3. If (9) holds for any N and h_1, \dots, h_N , then

$$\text{constant} \leq \frac{1}{2\pi} \int_0^{2\pi} \max_{w \in \mathcal{W}} \langle e^{j\theta}, w \rangle d\theta. \quad (42)$$

Proof. See App. C. \square

Although Thm. 3 affirms that the constant in (25) cannot be further tightened, it is, at its heart, a worst-case analysis. (In some cases, e.g., \mathcal{W} intersecting with the unit circle and $h_1 = \dots = h_n$, the ideal beamforming gain can even be attained.) Transcending the notion of worst case to embrace other notions, say the average beamforming gain, requires accepting that the channel is an instance of a fading distribution.

F. Fading Channels

Let us posit that $\{h_n\}$ are drawn from an i.i.d. circularly symmetric distribution, say they are i.i.d. realizations of h with $\mathbb{E}[|h|] < \infty$. As N grows large, light can be shed on the beamforming gain that goes beyond its worst-case value. Specifically, as formalized next, the bound established in Thm. 1 (with both sides normalized by N to keep it from diverging) becomes tight, in the sense that both sides converge to the same nonrandom limit

$$\mathbb{E}[|h|] \cdot \frac{1}{2\pi} \int_0^{2\pi} \max_{w \in \mathcal{W}} \langle e^{j\theta}, w \rangle d\theta. \quad (43)$$

Theorem 4. For $N \rightarrow \infty$, the sequence of random variables $\frac{g_{\mathcal{W}}}{N}$ converges almost surely (a.s.) to (43).

Proof. See App. D. \square

The expression in (11) therefore represents, for large N , not only the worst-case shortfall, but actually the shortfall attained a.s. for every channel realization. And, as formalized next, it also represents the average shortfall under the sole proviso that, as dictated by physics, $\mathbb{E}[|h|^2] < \infty$.

Theorem 5. If $\mathbb{E}[|h|^p] < \infty$ for some $p \geq 1$, the sequence of random variables $\frac{g_{\mathcal{W}}}{N}$ converges in mean of order p to (43),

$$\frac{\mathbb{E}[g_{\mathcal{W}}^p]}{N^p} \rightarrow (\mathbb{E}[|h|])^p \cdot \left(\frac{1}{2\pi} \int_0^{2\pi} \max_{w \in \mathcal{W}} \langle e^{j\theta}, w \rangle d\theta \right)^p. \quad (44)$$

Proof. See App. E. \square

For $p = 2$, the above result implies that the shortfall in average beamforming gain abides by (11).

IV. A GEOMETRIC PROOF

This section provides an alternative perspective on the problem. Following [31], one can recast

$$\max_{\mathbf{w} \in \mathcal{W}^N} \left| \sum_n w_n h_n \right| \quad (45)$$

as

$$\begin{aligned} \max_w |w| \\ \text{s.t. } w \in h_1 \mathcal{W} + \cdots + h_N \mathcal{W}, \end{aligned} \quad (46)$$

where the summations are Minkowski sums of sets. By means of Lemma 3 presented below, this can be reformulated as

$$\begin{aligned} \max_w |w| \\ \text{s.t. } w \in \text{Conv}(h_1 \mathcal{W} + \cdots + h_N \mathcal{W}). \end{aligned} \quad (47)$$

Lemma 3. For any compact set $S \subset \mathbb{C}$,

$$\max_{w \in S} |w| = \max_{w \in \text{Conv } S} |w|. \quad (48)$$

Proof. See App. F. \square

In turn, the Cauchy's surface area formula paves the way for two other results of interest.

Corollary 1. For compact convex sets S_1 and S_2 in \mathbb{C} ,

$$\text{perimeter of } S_1 + S_2 = \text{perimeter of } S_1 + \text{perimeter of } S_2.$$

Proof. See App. G. \square

Corollary 2. Given two compact convex sets S_1 and S_2 , if $S_1 \subset S_2 \subset \mathbb{C}$, the perimeter of S_1 is at most that of S_2 .

Proof. Since, on any direction, the width of S_1 is at most that of S_2 , the result follows from the Cauchy's surface area formula. \square

Armed with these corollaries, the main result in (9)–(10) can be proved in an alternative fashion. As per Lemma 2,

$$\begin{aligned} \text{Conv}(h_1 \mathcal{W} + \cdots + h_N \mathcal{W}) \\ = h_1 \text{Conv } \mathcal{W} + \cdots + h_N \text{Conv } \mathcal{W} \end{aligned} \quad (49)$$

and, applying repeatedly Cor. 1, we have that

$$\text{perimeter of } h_1 \text{Conv } \mathcal{W} + \cdots + h_N \text{Conv } \mathcal{W} \quad (50)$$

$$= \text{perimeter of } h_1 \text{Conv } \mathcal{W} + \cdots + \text{perimeter of } h_N \text{Conv } \mathcal{W}$$

$$= \sum_n \text{perimeter of } \text{Conv } \mathcal{W} \cdot |h_n| \quad (51)$$

$$= \text{perimeter of } \text{Conv } \mathcal{W} \cdot \sum_n |h_n| \quad (52)$$

$$= \text{perimeter of } \text{Conv } \mathcal{W} \cdot g_{\text{ideal}}. \quad (53)$$

As the optimal objective of (47) is g_{ideal} , (49) is contained in the disk $\{z \in \mathbb{C} : |z| \leq g_{\mathcal{W}}\}$. Applying Cor. 2, one obtains

$$2\pi g_{\mathcal{W}} = \text{perimeter of } \{z \in \mathbb{C} : |z| \leq g_{\mathcal{W}}\} \quad (54)$$

$$\geq \text{perimeter of } h_1 \text{Conv } \mathcal{W} + \cdots + h_N \text{Conv } \mathcal{W} \quad (55)$$

$$= \text{perimeter of } \text{Conv } \mathcal{W} \cdot g_{\text{ideal}}. \quad (56)$$

This geometric proof also provides intuition on why Thm. 3 must hold. From the reformulation in (47), the set (49) has an element whose modulus is $g_{\mathcal{W}}$. For $h_n = e^{j \frac{2\pi n}{N}}$, this set,

$$e^{j \frac{2\pi \cdot 1}{N}} \text{Conv } \mathcal{W} + e^{j \frac{2\pi \cdot 2}{N}} \text{Conv } \mathcal{W} + \cdots + e^{j \frac{2\pi \cdot N}{N}} \text{Conv } \mathcal{W},$$

is invariant under $\frac{2\pi}{N}$ -rotation. From this rotational invariance and the convexity, (49) includes a regular N -gon inscribed in

a disk of radius $g_{\mathcal{W}}$. By means of Cor. 2, (53) is bounded below by the perimeter of $\text{Conv } \mathcal{W}_N \cdot g_{\mathcal{W}}$, meaning that perimeter of $\text{Conv } \mathcal{W} \cdot g_{\text{ideal}} \geq \text{perimeter of } \text{Conv } \mathcal{W}_N \cdot g_{\mathcal{W}}$. Letting $N \rightarrow \infty$, the above becomes

$$g_{\mathcal{W}} \leq \frac{\text{perimeter of } \text{Conv } \mathcal{W}}{2\pi} \cdot g_{\text{ideal}} \quad (57)$$

for $h_n = e^{j \frac{2\pi n}{N}}$, which reaffirms Thm. 3.

A special case of the foregoing geometric proof, corresponding to $\mathcal{W} = \{0, 1\}$ as per (28), is given in [53, Thm. 3], in a derivation attributed to S. Kakutani.

V. A MINUTE TIGHTENING

According to Thm. 3, the obtained constant is optimal in the sense of the bound holding for any N . For a specific N , though, there is room for some slight further tightening when $\text{Conv } \mathcal{W}$ is a polygon. Indeed, for each N one can determine the constant satisfying (9) for any h_1, \dots, h_N and, as N grows, this constant decreases monotonically and converges to (10). A bound on this constant for specific N is given next.

Theorem 6. Provided that $\text{Conv } \mathcal{W}$ is a polygon with M vertices, (9) holds with the constant

$$\frac{\text{perimeter of } \text{Conv } \mathcal{W}}{\text{perimeter of } \text{Conv } \mathcal{W}_{MN}} = \frac{\text{perimeter of } \text{Conv } \mathcal{W}}{2MN \sin \frac{\pi}{MN}}. \quad (58)$$

Proof. See App. H. \square

The maximum discrepancy between (10) and (58), pertaining to the case $M = N = 2$, amounts to 0.9-dB difference in beamforming gain.

For the special case of a regular M -gon, $\mathcal{W} = \mathcal{W}_M$, the constant in (58) cannot be improved upon and it reduces to

$$\frac{\sin \frac{\pi}{M}}{N \sin \frac{\pi}{MN}}, \quad (59)$$

which generalizes the result proved in [61, Thm. 3.1] for \mathcal{W}_2 . As N grows large, the above reverts as anticipated to (10), which, for a regular M -gon, adopts the form

$$\frac{M}{\pi} \sin \frac{\pi}{M}. \quad (60)$$

This formula returns shortfalls of -3.9 dB, -0.9 dB, and -0.2 dB, respectively for 1-bit, 2-bit, and 3-bit discrete uniform phase shifters.

Beyond the realm of polygons, the best constant can also be determined for $\mathcal{W} = \{0, 1\}$ in some cases. It is $\frac{1}{2}$ for $N = 2$, and $\frac{1}{3}$ for $N = 3$ obtained from a trivial bound

$$\max_{w \in \{0, 1\}^N} \left| \sum_n w_n h_n \right| \geq \max_n |h_n| \geq \frac{1}{N} \sum_n |h_n|. \quad (61)$$

VI. CONCLUSION

Given any arbitrary set of feasible phase shifts, (11) quantifies the maximum penalty in transmit or receive beamforming gain, or in RIS-assisted beamforming gain, relative to ideality. In i.i.d. fading channels, the penalty concentrates to its maximum as the number of antennas grows. As potential follow-up work, one could entertain the generalization to correlated fading channels, in particular the assessment of whether (11) continues to hold.

VII. ACKNOWLEDGMENT

Heedong Do would like to recognize [55, Exercise 14.9], which brought [52] to his attention.

APPENDIX A

For any $h_0, \dots, h_N \in \mathbb{C}$,

$$\begin{aligned} \max_{(w_0, \mathbf{w}) \in \mathcal{W}_M^{N+1}} & \left| w_0 h_0 + \sum_n w_n h_n \right| \\ &= \max_{(w_0, \mathbf{w}) \in \mathcal{W}_M^{N+1}} \left| h_0 + \sum_n \frac{w_n}{w_0} h_n \right| \quad (62) \end{aligned}$$

$$\leq \max_{\mathbf{w} \in \mathcal{W}_M^N} \left| h_0 + \sum_n w_n h_n \right|, \quad (63)$$

where the inequality holds because $\left\{ \frac{w_n}{w_0} : w_0, w_n \in \mathcal{W} \right\} = \mathcal{W}$. The inequality in the reverse direction trivially holds.

APPENDIX B

Recalling (20),

$$\max_{\mathbf{w} \in \mathcal{W}^N} \left| \sum_n w_n h_n \right| = \max_{\theta \in [0, 2\pi]} \sum_n |h_n| \max_{w \in \mathcal{W}} \langle e^{j(\theta - \theta_n)}, w \rangle. \quad (64)$$

As the maximum is at least the average, a lower bound is given by

$$\begin{aligned} \frac{1}{2\pi} \int_0^{2\pi} \sum_n |h_n| \max_{w \in \mathcal{W}} \langle e^{j(\theta - \theta_n)}, w \rangle d\theta \\ = \sum_n |h_n| \cdot \frac{1}{2\pi} \int_0^{2\pi} \max_{w \in \mathcal{W}} \langle e^{j(\theta - \theta_n)}, w \rangle d\theta. \quad (65) \end{aligned}$$

From the periodicity of (24), it holds that

$$\frac{1}{2\pi} \int_0^{2\pi} \max_{w \in \mathcal{W}} \langle e^{j(\theta - \theta_n)}, w \rangle d\theta = \frac{1}{2\pi} \int_0^{2\pi} \max_{w \in \mathcal{W}} \langle e^{j\theta}, w \rangle d\theta \quad (66)$$

for all n . This turns (65) into

$$\frac{1}{2\pi} \int_0^{2\pi} \max_{w \in \mathcal{W}} \langle e^{j\theta}, w \rangle d\theta \cdot \sum_n |h_n|, \quad (67)$$

as desired.

APPENDIX C

It suffices to find one concrete such N and h_1, \dots, h_N . For a given N , let

$$h_n = e^{j \frac{2\pi n}{N}}. \quad (68)$$

The strategy shall be letting $N \rightarrow \infty$ on both sides of

$$\frac{1}{N} \max_{\mathbf{w} \in \mathcal{W}^N} \left| \sum_n w_n h_n \right| \geq \text{constant} \cdot \frac{1}{N} \sum_n |h_n|. \quad (69)$$

From (20), the left-hand side equals

$$\max_{\theta \in [0, 2\pi]} \frac{1}{N} \sum_n \max_{w \in \mathcal{W}} \langle e^{j(\theta - \frac{2\pi n}{N})}, w \rangle. \quad (70)$$

As (24) is a continuous function over a compact set, it is uniformly continuous [62, Thm. 4.42]. Therefore, the convergence

$$\frac{1}{N} \sum_n \max_{w \in \mathcal{W}} \langle e^{j(\theta - \frac{2\pi n}{N})}, w \rangle \rightarrow \frac{1}{2\pi} \int_0^{2\pi} \max_{w \in \mathcal{W}} \langle e^{j\theta}, w \rangle d\theta$$

is uniform [62, Exercise 4.51]. For $N \rightarrow \infty$, the left-hand side of (69) becomes

$$\begin{aligned} \lim_{N \rightarrow \infty} \max_{\theta \in [0, 2\pi]} \frac{1}{N} \sum_n \max_{w \in \mathcal{W}} \langle e^{j(\theta - \frac{2\pi n}{N})}, w \rangle \\ = \max_{\theta \in [0, 2\pi]} \lim_{N \rightarrow \infty} \frac{1}{N} \sum_n \max_{w \in \mathcal{W}} \langle e^{j(\theta - \frac{2\pi n}{N})}, w \rangle \quad (71) \end{aligned}$$

$$= \max_{\theta \in [0, 2\pi]} \frac{1}{2\pi} \int_0^{2\pi} \max_{w \in \mathcal{W}} \langle e^{j\theta}, w \rangle d\theta \quad (72)$$

$$= \frac{1}{2\pi} \int_0^{2\pi} \max_{w \in \mathcal{W}} \langle e^{j\theta}, w \rangle d\theta, \quad (73)$$

where the limit and the maximum can be interchanged thanks to the uniform convergence. As of the right-hand side of (69), it directly equals the constant because, in light of (68), $\frac{1}{N} \sum_n |h_n| = 1$. Altogether,

$$\frac{1}{2\pi} \int_0^{2\pi} \max_{w \in \mathcal{W}} \langle e^{j\theta}, w \rangle d\theta \geq \text{constant} \quad (74)$$

as desired.

APPENDIX D

Recalling (20), it suffices to show that

$$\frac{g_{\mathcal{W}}}{N} = \max_{\theta \in [0, 2\pi]} \frac{1}{N} \sum_n |h_n| \max_{w \in \mathcal{W}} \langle e^{j(\theta - \theta_n)}, w \rangle \quad (75)$$

$$\xrightarrow{\text{a.s.}} \mathbb{E}[|h|] \cdot \frac{1}{2\pi} \int_0^{2\pi} \max_{w \in \mathcal{W}} \langle e^{j\theta}, w \rangle d\theta. \quad (76)$$

To that purpose, let us render explicit the sample space Ω , on which the random variables h_1, h_2, \dots and $\theta_1, \theta_2, \dots$ live, and its probability function P . The goal here is to find $\Omega' \subset \Omega$ satisfying $P(\Omega') = 1$ and

$$\begin{aligned} \max_{\theta \in [0, 2\pi]} \frac{1}{N} \sum_n |h_n(\omega)| \max_{w \in \mathcal{W}} \langle e^{j(\theta - \theta_n(\omega))}, w \rangle \\ \rightarrow \mathbb{E}[|h|] \cdot \frac{1}{2\pi} \int_0^{2\pi} \max_{w \in \mathcal{W}} \langle e^{j\theta}, w \rangle d\theta \end{aligned} \quad (77)$$

for any $\omega \in \Omega'$.

From the strong law of large numbers [63, Cor. 5.2.1], for every $\theta \in [0, 2\pi]$ there exists $\Omega_\theta \subset \Omega$ satisfying $P(\Omega_\theta) = 1$ and

$$\begin{aligned} \frac{1}{N} \sum_n |h_n(\omega)| \max_{w \in \mathcal{W}} \langle e^{j(\theta - \theta_n(\omega))}, w \rangle \\ \rightarrow \mathbb{E}[|h|] \cdot \frac{1}{2\pi} \int_0^{2\pi} \max_{w \in \mathcal{W}} \langle e^{j\theta}, w \rangle d\theta \end{aligned} \quad (78)$$

for any $\omega \in \Omega_\theta$. Repeating the argument, we also have $A \subset \Omega$ such that $P(A) = 1$ and

$$\frac{1}{N} \sum_n |h_n(\omega)| \rightarrow \mathbb{E}[|h|]. \quad (79)$$

As a countable intersection of events of probability one is itself of probability one [63, Exercise 1.5.5], $P(\Omega') = 1$ with

$$\Omega' = A \cap \bigcap_{\theta \in [0, 2\pi] \cap \mathbb{Q}} \Omega_\theta. \quad (80)$$

For $\omega \in \Omega'$ fixed, one can think of the left-hand side of (78),

$$\frac{1}{N} \sum_n |h_n(\omega)| \max_{w \in \mathcal{W}} \langle e^{j(\theta - \theta_n(\omega))}, w \rangle, \quad (81)$$

as a sequence of functions of θ . Two properties of (81) come in handy:

- 1) By construction, for $\theta \in [0, 2\pi] \cap \mathbb{Q}$, (81) converges pointwisely to the nonrandom limit,

$$\mathbb{E}[|h|] \cdot \frac{1}{2\pi} \int_0^{2\pi} \max_{w \in \mathcal{W}} \langle e^{j\theta}, w \rangle d\theta. \quad (82)$$

- 2) Each summand in (81) is Lipschitz continuous as

$$\left| \max_{w \in \mathcal{W}} \langle e^{j\theta}, w \rangle - \max_{w \in \mathcal{W}} \langle e^{j\theta'}, w \rangle \right| \quad (83)$$

$$\leq \left| \max_{w \in \mathcal{W}} \left(\langle e^{j\theta}, w \rangle - \langle e^{j\theta'}, w \rangle \right) \right| \quad (84)$$

$$= \left| \max_{w \in \mathcal{W}} \langle e^{j\theta} - e^{j\theta'}, w \rangle \right| \quad (85)$$

$$\leq |e^{j\theta} - e^{j\theta'}| \max_{w \in \mathcal{W}} |w| \quad (86)$$

$$\leq |\theta - \theta'| \max_{w \in \mathcal{W}} |w|. \quad (87)$$

Therefore, (81) is a function with Lipschitz constant

$$\max_{w \in \mathcal{W}} |w| \cdot \frac{1}{N} \sum_n |h_n(\omega)|. \quad (88)$$

From (79) and the fact that a convergent sequence is bounded, (88) is bounded above. This means the sequence of functions in (81) is equicontinuous [62, Exercise 4.15].

These two observations allow for the application of the Arzelà-Ascoli propagation theorem [62, Thm. 4.16], extending the pointwise convergence over $[0, 2\pi] \cap \mathbb{Q}$ to the uniform convergence over $[0, 2\pi]$. This proves (76) and, with that, the convergence of $\frac{g_{\mathcal{W}}}{N}$ to (43).

APPENDIX E

From [63, Example 4.3.1], given that $\{|h_n|\}$ are i.i.d. random variables with $\mathbb{E}[|h|^p] < \infty$,

$$\left(\frac{g_{\text{ideal}}}{N} \right)^p = \left(\frac{1}{N} \sum_n |h_n| \right)^p \quad (89)$$

is uniformly integrable. As

$$0 \leq \left(\frac{g_{\mathcal{W}}}{N} \right)^p \leq \left(\frac{g_{\text{ideal}}}{N} \right)^p, \quad (90)$$

$\left(\frac{g_{\mathcal{W}}}{N} \right)^p$ is uniformly integrable as well [63, pp. 94]. In conjunction with the convergence in probability, implied by the a.s. convergence [63, Cor. 3.3.1], $\left(\frac{g_{\mathcal{W}}}{N} \right)^p$ converges in mean of order p to the same limit [63, Thm. 4.2.3].

APPENDIX F

Although the proof can be found in [31, Lemma 1], it is derived here concisely as a direct consequence of Lemma 1:

$$\max_{w \in S} |w| = \max_{w \in S} \max_{\theta \in [0, 2\pi]} \langle e^{j\theta}, w \rangle \quad (91)$$

$$= \max_{\theta \in [0, 2\pi]} \max_{w \in S} \langle e^{j\theta}, w \rangle \quad (92)$$

$$= \max_{\theta \in [0, 2\pi]} \max_{w \in \text{Conv } S} \langle e^{j\theta}, w \rangle \quad (93)$$

$$= \max_{w \in \text{Conv } S} \max_{\theta \in [0, 2\pi]} \langle e^{j\theta}, w \rangle \quad (94)$$

$$= \max_{w \in \text{Conv } S} |w|. \quad (95)$$

APPENDIX G

Applying the Cauchy's surface area formula and Lemma 4 (presented below), we have that

perimeter of $S_1 + S_2$

$$= \int_0^{2\pi} \max_{w \in S_1 + S_2} \langle e^{j\theta}, w \rangle d\theta \quad (96)$$

$$= \int_0^{2\pi} \max_{w \in S_1} \langle e^{j\theta}, w \rangle d\theta + \int_0^{2\pi} \max_{w \in S_2} \langle e^{j\theta}, w \rangle d\theta \quad (97)$$

$$= \text{perimeter of } S_1 + \text{perimeter of } S_2. \quad (98)$$

Lemma 4. For compact sets S_1 and S_2 in \mathbb{C} ,

$$\max_{w \in S_1 + S_2} \langle z, w \rangle = \max_{w \in S_1} \langle z, w \rangle + \max_{w \in S_2} \langle z, w \rangle. \quad (99)$$

Proof. See [50, Thm. 1.7.5]. \square

APPENDIX H

The proof is in essence identical to the geometric proof in Sec. IV. An additional observation is that (49) has at most $N|\mathcal{W}|$ vertices [64, Ch. 13.3]. Application of Lemma 5 (presented below) gives

$$2MN \sin \frac{\pi}{MN} \cdot g_{\mathcal{W}}$$

$$\geq \text{perimeter of } h_1 \text{Conv } \mathcal{W} + \cdots + h_N \text{Conv } \mathcal{W} \quad (100)$$

$$= \text{perimeter of } \text{Conv } \mathcal{W} \cdot g_{\text{ideal}}. \quad (101)$$

Equality holds if and only if $h_1 \text{Conv } \mathcal{W} + \cdots + h_N \text{Conv } \mathcal{W}$ forms the regular MN -gon. For $\mathcal{W} = \mathcal{W}_M$, $h_n = e^{j2\pi \frac{n}{MN}}$ for $n = 1, \dots, N$ satisfies this condition.

Lemma 5. Consider a convex polygon S with M vertices lying inside the unit circle. The perimeter of S is at most

$$\text{perimeter of } \mathcal{W}_M = 2M \sin \frac{\pi}{M}. \quad (102)$$

Proof. Although the proof is provided in [61, Prop. 2.1], it is repeated here for the sake of completeness. As the statement trivially holds for $M = 1$, it is assumed that $M \geq 2$. A point can then be found in S that is not an extreme point. Let us think of a ray emanating from that point to every vertex. A convex polygon can be constructed by taking the convex hull of the intersection of the rays and the unit circle (see Fig. 4). The perimeter of this polygon is at least that of the original polygon, from Cor. 2. With this observation, it suffices to

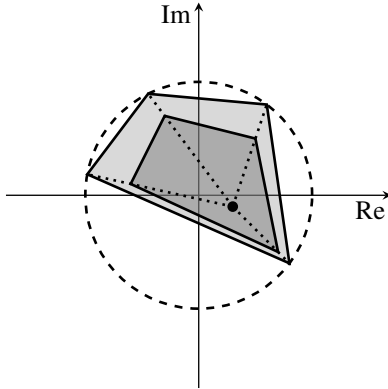


Fig. 4. Construction of a convex polygon whose perimeter is at least that of the original convex polygon.

consider the polygons whose vertices are on the unit circle. The perimeter can then be expressed as

$$2 \sum_{m=1}^M \sin \phi_m \quad (103)$$

with $\sum_{m=1}^M \phi_m = \pi$ and $\phi_m \geq 0$ for all m . Concavity of the sine function over $[0, \pi]$ concludes the proof. \square

REFERENCES

- [1] R. W. Heath, Jr. and A. Lozano, *Foundations of MIMO Communication*. Cambridge University Press, 2018.
- [2] Z. Wang, J. Zhang, H. Du, D. Niyato, S. Cui, B. Ai, M. Debbah, K. B. Letaief, and H. V. Poor, “A tutorial on extremely large-scale MIMO for 6G: Fundamentals, signal processing, and applications,” *IEEE Commun. Surv. Tut.*, vol. 26, no. 3, pp. 1560–1605, 2024.
- [3] A. Chakraborty and B. Gupta, “Paradigm phase shift: RF MEMS phase shifters: An overview,” *IEEE Microw. Mag.*, vol. 18, no. 1, pp. 22–41, 2017.
- [4] M. Fakharzadeh, P. Mousavi, S. Safavi-Naeini, and S. H. Jamali, “The effects of imbalanced phase shifters loss on phased array gain,” *IEEE Antennas Wireless Propag. Lett.*, vol. 7, pp. 192–196, 2008.
- [5] R. Mailloux, “Array grating lobes due to periodic phase, amplitude, and time delay quantization,” *IEEE Trans. Antennas Propag.*, vol. 32, no. 12, pp. 1364–1368, 1984.
- [6] L. Liang, W. Xu, and X. Dong, “Low-complexity hybrid precoding in massive multiuser MIMO systems,” *IEEE Wireless Commun. Lett.*, vol. 3, no. 6, pp. 653–656, 2014.
- [7] H. Yang, F. Yang, S. Xu, M. Li, X. Cao, J. Gao, and Y. Zheng, “A study of phase quantization effects for reconfigurable reflectarray antennas,” *IEEE Antennas Wireless Propag. Lett.*, vol. 16, pp. 302–305, 2017.
- [8] H. Do, N. Lee, and A. Lozano, “Line-of-sight MIMO via intelligent reflecting surface,” *IEEE Trans. Wireless Commun.*, vol. 22, no. 6, pp. 4215–4231, 2023.
- [9] S. Loyka and M. Dabiri, “IRS with discrete phase shifts: When is quantization optimal?” *IEEE Wireless Commun. Lett.*, vol. 14, no. 4, pp. 989–993, 2025.
- [10] R. Haupt, “Phase-only adaptive nulling with a genetic algorithm,” *IEEE Trans. Antennas Propag.*, vol. 45, no. 6, pp. 1009–1015, 1997.
- [11] T. H. Ismail and Z. M. Hamici, “Array pattern synthesis using digital phase control by quantized particle swarm optimization,” *IEEE Trans. Antennas Propag.*, vol. 58, no. 6, pp. 2142–2145, 2010.
- [12] S. Goudos, “Antenna design using binary differential evolution: Application to discrete-valued design problems,” *IEEE Antennas Propag. Mag.*, vol. 59, no. 1, pp. 74–93, 2017.
- [13] M. K. Leino, J. Bergman, J. Ala-Laurinaho, and V. Viikari, “Beam optimization for 28 GHz phased array utilizing measurement data,” in *Eur. Conf. Antennas Propag.*, 2020.
- [14] S. Madani, S. Jog, J. O. Lacruz, J. Widmer, and H. Hassanieh, “Practical null steering in millimeter wave networks,” in *USENIX Symp. Networked Systems Design Implementation*, 2021, pp. 903–921.
- [15] A. Narula, M. Lopez, M. Trott, and G. Wornell, “Efficient use of side information in multiple-antenna data transmission over fading channels,” *IEEE J. Sel. Areas Commun.*, vol. 16, no. 8, pp. 1423–1436, 1998.
- [16] R. Heath and A. Paulraj, “A simple scheme for transmit diversity using partial channel feedback,” in *Asilomar Conf. Signals Syst. Comput.*, vol. 2, 1998, pp. 1073–1078.
- [17] D. Love and R. Heath, “Equal gain transmission in multiple-input multiple-output wireless systems,” *IEEE Trans. Commun.*, vol. 51, no. 7, pp. 1102–1110, 2003.
- [18] C. R. Murthy and B. D. Rao, “Quantization methods for equal gain transmission with finite rate feedback,” *IEEE Trans. Signal Process.*, vol. 55, no. 1, pp. 233–245, 2007.
- [19] S.-H. Tsai, “Transmit equal gain precoding in Rayleigh fading channels,” *IEEE Trans. Signal Process.*, vol. 57, no. 9, pp. 3717–3721, 2009.
- [20] K. Mackenthun, “A fast algorithm for multiple-symbol differential detection of MPSK,” *IEEE Trans. Commun.*, vol. 42, no. 234, pp. 1471–1474, 1994.
- [21] W. Sweldens, “Fast block noncoherent decoding,” *IEEE Commun. Lett.*, vol. 5, no. 4, pp. 132–134, 2001.
- [22] I. Motedad-Aval and A. Anastopoulos, “Polynomial-complexity noncoherent symbol-by-symbol detection with application to adaptive iterative decoding of turbo-like codes,” *IEEE Trans. Commun.*, vol. 51, no. 2, pp. 197–207, 2003.
- [23] P. N. Alevizos, Y. Fountoulas, G. N. Karystinos, and A. Bletsas, “Log-linear-complexity GLRT-optimal noncoherent sequence detection for orthogonal and RFID-oriented modulations,” *IEEE Trans. Commun.*, vol. 64, no. 4, pp. 1600–1612, 2016.
- [24] J. Deng, O. Tirkkonen, and C. Studer, “MmWave multiuser MIMO precoding with fixed subarrays and quantized phase shifters,” *IEEE Trans. Veh. Technol.*, vol. 68, no. 11, pp. 11132–11145, 2019.
- [25] J. Sanchez, E. Bengtsson, F. Rusek, J. Flordelis, K. Zhao, and F. Tufvesson, “Optimal, low-complexity beamforming for discrete phase reconfigurable intelligent surfaces,” in *IEEE Global Commun. Conf.*, 2021.
- [26] Y. Zhang, K. Shen, S. Ren, X. Li, X. Chen, and Z.-Q. Luo, “Configuring intelligent reflecting surface with performance guarantees: Optimal beamforming,” *IEEE J. Sel. Topics Signal Process.*, vol. 16, no. 5, pp. 967–979, 2022.
- [27] S. Ren, K. Shen, X. Li, X. Chen, and Z.-Q. Luo, “A linear time algorithm for the optimal discrete IRS beamforming,” *IEEE Wireless Commun. Lett.*, vol. 12, no. 3, pp. 496–500, 2023.
- [28] I. Vardakis, G. Kotridis, S. Peppas, K. Skyvalakis, G. Vougioukas, and A. Bletsas, “Intelligently wireless batteryless RF-powered reconfigurable surface: Theory, implementation & limitations,” *IEEE Trans. Wireless Commun.*, vol. 22, no. 6, pp. 3942–3954, 2023.
- [29] D. K. Pekcan and E. Ayanoglu, “Achieving optimum received power for discrete-phase RISs with elementwise updates in the least number of steps,” *IEEE Open J. Commun. Soc.*, vol. 5, pp. 2706–2722, 2024.
- [30] S. Sanjay Narayanan, U. K. Khankhoje, and R. Krishna Ganti, “Optimum beamforming and grating-lobe mitigation for intelligent reflecting surfaces,” *IEEE Trans. Antennas Propag.*, vol. 72, no. 11, pp. 8540–8553, 2024.
- [31] H. Do and A. Lozano, “Optimum discrete beamforming via Minkowski sum of polygons,” 2026. [Online]. Available: <https://arxiv.org/abs/2512.15546>
- [32] S. Zhang, C. Guo, T. Wang, and W. Zhang, “ON-OFF analog beamforming for massive MIMO,” *IEEE Trans. Veh. Technol.*, vol. 67, no. 5, pp. 4113–4123, 2018.
- [33] V. Arun and H. Balakrishnan, “RFocus: Beamforming using thousands of passive antennas,” in *USENIX Symp. Networked Syst. Design Implementation*, 2020, pp. 1047–1061.
- [34] A. Khaleel and E. Basar, “Phase shift-free passive beamforming for reconfigurable intelligent surfaces,” *IEEE Trans. Commun.*, vol. 70, no. 10, pp. 6966–6976, 2022.
- [35] S. Nassirpour, A. Gupta, A. Vahid, and D. Bharadia, “Power-efficient analog front-end interference suppression with binary antennas,” *IEEE Trans. Wireless Commun.*, vol. 22, no. 4, pp. 2592–2605, 2023.
- [36] M. Smith and Y. Guo, “A comparison of methods for randomizing phase quantization errors in phased arrays,” *IEEE Trans. Antennas Propag.*, vol. 31, no. 6, pp. 821–828, 1983.
- [37] F. Sohrabi and W. Yu, “Hybrid digital and analog beamforming design for large-scale antenna arrays,” *IEEE J. Sel. Topics Signal Process.*, vol. 10, no. 3, pp. 501–513, 2016.
- [38] Z. Wang, M. Li, Q. Liu, and A. L. Swindlehurst, “Hybrid precoder and combiner design with low-resolution phase shifters in mmWave MIMO systems,” *IEEE J. Sel. Topics Signal Process.*, vol. 12, no. 2, pp. 256–269, 2018.

- [39] Q. Wu and R. Zhang, "Beamforming optimization for wireless network aided by intelligent reflecting surface with discrete phase shifts," *IEEE Trans. Commun.*, vol. 68, no. 3, pp. 1838–1851, 2020.
- [40] L. Cao, H. Yin, L. Tan, and X. Pei, "RIS with insufficient phase shifting capability: Modeling, beamforming, and experimental validations," *IEEE Trans. Commun.*, vol. 72, no. 9, pp. 5911–5923, 2024.
- [41] D. Kutay Pekcan, H. Liao, and E. Ayanoglu, "Received power maximization using nonuniform discrete phase shifts for RISs with a limited phase range," *IEEE Open J. Commun. Soc.*, vol. 5, pp. 7447–7466, 2024.
- [42] H. Xu, H. Wei, H. Chen, Z. Chen, X. Zhou, H. Xu, and Y. Quan, "Effect of periodic phase modulation on the matched filtering with insufficient phase-shift capability," *IEEE Trans. Aerosp. Electron. Syst.*, vol. 61, no. 3, pp. 5755–5770, 2025.
- [43] N. Shlezinger, O. Dicker, Y. C. Eldar, I. Yoo, M. F. Imani, and D. R. Smith, "Dynamic metasurface antennas for uplink massive MIMO systems," *IEEE Trans. Commun.*, vol. 67, no. 10, pp. 6829–6843, 2019.
- [44] M. Rezvani and R. Adve, "Channel estimation for dynamic metasurface antennas," *IEEE Trans. Wireless Commun.*, vol. 23, no. 6, pp. 5832–5846, 2024.
- [45] M. R. Castellanos, S. Yang, C.-B. Chae, and R. W. Heath, "Embracing reconfigurable antennas in the tri-hybrid MIMO architecture for 6G and beyond," *IEEE Trans. Commun.*, pp. 1–1, 2025.
- [46] B. Di, H. Zhang, L. Song, Y. Li, Z. Han, and H. V. Poor, "Hybrid beamforming for reconfigurable intelligent surface based multi-user communications: Achievable rates with limited discrete phase shifts," *IEEE J. Sel. Areas Commun.*, vol. 38, no. 8, pp. 1809–1822, 2020.
- [47] S. Abeywickrama, R. Zhang, Q. Wu, and C. Yuen, "Intelligent reflecting surface: Practical phase shift model and beamforming optimization," *IEEE Trans. Commun.*, vol. 68, no. 9, pp. 5849–5863, 2020.
- [48] Y. Zhang, J. Zhang, M. D. Renzo, H. Xiao, and B. Ai, "Performance analysis of RIS-aided systems with practical phase shift and amplitude response," *IEEE Trans. Veh. Technol.*, vol. 70, no. 5, pp. 4501–4511, 2021.
- [49] R. T. Rockafellar, *Convex analysis*. Princeton university press, 1997, vol. 11.
- [50] R. Schneider, *Convex bodies: the Brunn–Minkowski theory*. Cambridge university press, 2013.
- [51] R. P. Kaufman and N. W. Rickert, "An inequality concerning measures," *Bull. Amer. Math. Soc.*, vol. 72, no. 4, pp. 672–676, 1966.
- [52] W. Bledsoe, "An inequality about complex numbers," *Amer. Math. Monthly*, vol. 77, no. 2, pp. 180–182, 1970.
- [53] D. Daykin and A. Wilansky, "Sets of complex numbers," *Math. Mag.*, vol. 47, no. 4, pp. 228–229, 1974.
- [54] N. Bourbaki, *General topology: chapters 5–10*. Springer, 1966.
- [55] J. M. Steele, *The Cauchy-Schwarz master class: an introduction to the art of mathematical inequalities*. Cambridge University Press, 2004.
- [56] A. Liu, *Chinese Mathematics Competitions and Olympiads 1981–1993*. Australian Mathematics Trust, 1998, vol. 13.
- [57] V. Vouk, "Projected area of convex bodies," *Nature*, vol. 162, no. 4113, pp. 330–331, 1948.
- [58] B. Meltzer, "Shadow area of convex bodies," *Nature*, vol. 163, no. 4136, pp. 220–220, 1949.
- [59] Y. Han, W. Tang, S. Jin, C.-K. Wen, and X. Ma, "Large intelligent surface-assisted wireless communication exploiting statistical CSI," *IEEE Trans. Veh. Technol.*, vol. 68, no. 8, pp. 8238–8242, 2019.
- [60] R. Mailloux, "Phased array theory and technology," *Proc. IEEE*, vol. 70, no. 3, pp. 246–291, 1982.
- [61] F. Grunbacher, "A sharp bound on large planar signed vector sums," 2025. [Online]. Available: <https://arxiv.org/abs/2502.13752>
- [62] C. C. Pugh, *Real mathematical analysis*, 2nd ed. Springer, 2015.
- [63] Y. S. Chow and H. Teicher, *Probability theory: independence, interchangeability, martingales*, 3rd ed. Springer Science & Business Media, 1997.
- [64] M. De Berg, O. Cheong, M. Van Kreveld, and M. Overmars, *Computational geometry: algorithms and applications*, 3rd ed. Springer, 2008.